SCIENCE CHINA
Physics, Mechanics & Astronomy

•Article•

July 2020 Vol. 63 No. 7: 276111
https://doi.org/10.1007/s11433-020-1539-4

Revisiting the breakdown of Stokes-Einstein relation in glass-forming liquids with machine learning

ZhenWei Wu[1*†], and Renzhong Li[2†]

[1] *School of Systems Science, Beijing Normal University, Beijing 100875, China;*
[2] *International Center for Quantum Materials and School of Physics, Peking University, Beijing 100871, China*

Received January 16, 2020; accepted March 5, 2020; published online March 25, 2020

The Stokes-Einstein (SE) relation has been considered as one of the hallmarks of dynamics in liquids. It describes that the diffusion constant D is proportional to $(\tau/T)^{-1}$, where τ is the structural relaxation time and T is the temperature. In many glass-forming liquids, the breakdown of SE relation often occurred when the dynamics of the liquids becomes glassy, and its origin is still debated among many scientists. Using molecular dynamics simulations and support-vector machine method, it is found that the scaling between diffusion and relaxation fails when the total population of solid-like clusters shrinks at the maximal rate with decreasing temperature, which implies a dramatic unification of clusters into an extensive dominant one occurs at the time of breakdown of the SE relation. Our data leads to an interpretation that the SE violation in metallic glass-forming liquids can be attributed to a specific change in the atomic structures.

metallic glass-forming liquid, machine learning, Stokes-Einstein relation

PACS number(s): 64.70.pe, 61.20.Ja, 66.20.Cy

Citation: Z. W. Wu, and R. Li, Revisiting the breakdown of Stokes-Einstein relation in glass-forming liquids with machine learning, Sci. China-Phys. Mech. Astron. **63**, 276111 (2020), https://doi.org/10.1007/s11433-020-1539-4

1 Introduction

The understanding of the dynamic properties of supercooled liquids for metallic alloys is of crucial importance in condensed matter physics and material science [1-3]. When a liquid is supercooled below its melting temperature, the characteristic timescales of its dynamics become obviously rich, bridging the gap between microscopic oscillation times and macroscopic relaxation times [4-7]. Many interesting phenomena occur during the vitrification process, such as dynamic heterogeneity, super Arrhenius behavior and a breakdown of Stokes-Einstein (SE) relation. The SE relation expresses the transport coefficient D in relation to the structural relaxation time τ and temperature T, which is represented as $D \propto (\tau / T)^{-1}$. The SE relation is valid for most liquids at a broad range of high temperatures but in contrast, at supercooled temperatures, especially near glass transition temperature, the SE relation is not observed [8-11].

As one of the most important anomalies that has been reported in different types of supercooled liquids, the origin of the breakdown of the SE relation has attracted a lot of attentions [8-16]. No conclusion has been reached in this regard and also the physical mechanism remains elusive especially for metallic glass-forming liquid systems with no apparent density anomaly unlike water [11], silica, and silicon [12]. For instance, some studies reported that dynamic heterogeneity (that is particles having distinct high and low mobility) gives rise to the breakdown of the SE relation [13,14]. However, Becker et al. [15] reported that both mo-

---

*Corresponding author (email: zwwu@bnu.edu.cn)
†These authors contributed equally to this work.

bile and immobile particles violate the SE relation in a network-forming liquid. Concurrently, SE relation breakdown has been associated with the structural change of liquid. Soklaski et al. [10] suggested that there exists a relation between the breakdown of the SE relation and the locally preferred structures; Xu et al. [11] also reported an obvious change of tetrahedral-like and non-tetrahedral-like structures in water at the temperature where the SE relation breaks down. Recently, Pan et al. [16] observed a correlation between the breakdown of the SE relation and the structural change of the clusters consisting of trapped atoms.

In this study, contrary to using a priori quantity such as local favorite structure or bond orientational order to look for correlations between structure and dynamics [17], we adopted the machine learning method [17,18] to investigate the relationship between spatial structure and dynamics as a model of metallic glass-forming alloy $Cu_{50}Zr_{50}$ was supercooled to form a glass. A training set is obtained from the molecular dynamics trajectory of “liquid-like” atoms in high-temperature liquid states and “solid-like” atoms in low-temperature glass states, and then the two categories were separated by a best-fit hyperplane using the support vector machine (SVM) method. This training model based on purely geometric information is deemed appropriately and employed in the classification of atoms into “liquid-like” or “solid-like” groups in the process of quenching. The SE violation is observed to have set in close to the transition temperature where the population of the separated solid-like clusters starts to decline with the fastest shrinking rate, which implies a dramatic unification of clusters into an extensive dominant one occurs at the time of SE relation breakdown. These results reveal changes in the dynamic behavior can be related to the corresponding formation of liquid structures.

2 Model and method

We performed classical molecular dynamics (MD) simulations with the LAMMPS package [19] to study the model system of $Cu_{50}Zr_{50}$ metallic glass-forming alloy. The atomic interactions for the system, including approximations of many-body interactions, are described by a realistic embedded-atom method potential [20]. The system contains 10000 atoms in a cubic box with periodic boundary conditions, and the MD step is 2 fs. An initial configuration of the alloy was generated randomly and then allowed to melt and evolve for 10 ns at 2000 K in the *NPT* ($P = 0$) ensemble with Nose-Hoover thermostat and barostat. Subsequently, the liquid sample was quenched to its target temperature at a cooling rate of 10^{12} K/s and then relaxed for 2 ns before structure and dynamics data were collected. The targeted temperatures for the computation of dynamics were in the range of 1500-1000 K. We also quenched the sample from 2000 to 300 K continuously at a cooling rate of 10^{12} K/s to study the evolution of local structures, and for the cooling rate effect, we studied the rate of 10^{11} and 10^{13} K/s, which returned almost the same results for the machine learning analysis.

The radial structure function defined in ref. [17] was applied to describe a particle’s local structural environment,

$$G_X(i;r,\delta) = \sum_{j\in X} \mathrm{e}^{-\frac{1}{2\delta^2}\left(r-R_{ij}\right)^2}, \tag{1}$$

where R_{ij} is the distance between particles i and j; X is the label that identifies the species of particles in the system; δ is the standard deviation parameter. Following the method of Schoenholz et al. [17], here we keep $\delta = 0.2$ Å fixed and take r to be between 2 Å and 10 Å in increments of 0.2 Å, which gives a total of 80 radial structure functions per particle. The local structural environment of a particle i is thus encoded as a point in a M-dimensional space (here $M = 80$). The SVM method then solves the classification problem by constructing a hyperplane in the high-dimensional vector space which best separates particles from one category (with label = 1) to another (label = 0). Having established the hyperplane for the training set “liquid-like” particles can be identified on the label = 1 class and “solid-like” particles fall into the other classification. The equilibrated 2000 K sample is relaxed for another 20 ns and 100 independent atomic configurations are collected as the set for label = 1. Subsequently, as the 300 K was achieved, the system was further relaxed for 20 ns at the same temperature and another 100 atomic configuration data obtained for the other set, label = 0. Using these configurations, we can construct the training set and testing set with the SVM method and subsequently get the appropriate model to distinguish the particles between liquid-like and solid-like (or say glass-like structurally) ones in the system during the quenching process.

3 Results and discussions

We initially determined the dynamic properties of the liquid and considered for each temperature the mean square displacement value, $\left\langle \Delta^2 r(t)\right\rangle$, and then used the Einstein relation to evaluate the corresponding diffusion coefficient for Cu atoms,

$$D = \lim_{t\to\infty}\frac{1}{6t}\left\langle \Delta^2 r(t)\right\rangle, \tag{2}$$

where $\langle . \rangle$ denotes the average overall particles and time origins. Figure 1(a) shows the mean-squared displacement as a function of time, and it can be seen that all the systems with a temperature range of 1000-1500 K entered into their diffusive regime. We also measured the self-intermediate

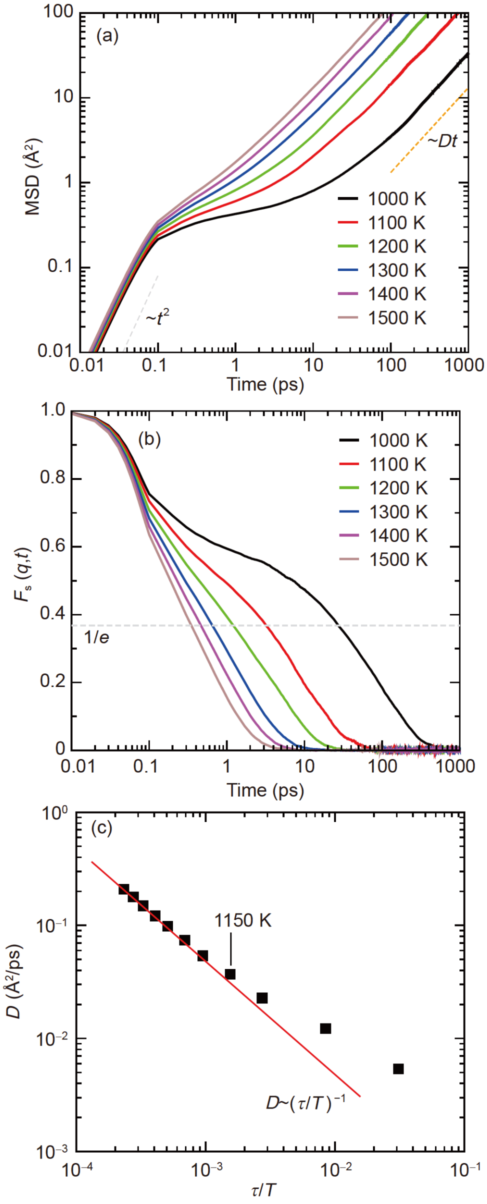

Figure 1 (Color online) (a) Mean-squared displacements and (b) self-intermediate scattering functions at temperatures ranged from 1500 to 1000 K in steps of 100 K. (c) Self-diffusion coefficient D as a function of structural relaxation time τ scaled by temperature T. The system follows the SE relation till to 1150 K and violates the SE relation below 1150 K.

scattering function [21] for these samples, which is defined as:

$$F_{\mathrm{S}}(q,t)=\frac{1}{N}\sum_{j=1}^{N}\left\langle \exp\left[-\mathrm{i}\mathbf{q}\cdot\left(\mathbf{r}_j(t)-\mathbf{r}_j(0)\right)\right]\right\rangle, \tag{3}$$

where N is the number of particles considered, $\langle.\rangle$ is the thermal average, and $\mathbf{r}_j(t)$ is the position of particle j at time t. The wave-vector is 2.8 Å^{-1} which corresponds to the main peak in the static structure factor [4]. The structural relaxation time τ is defined as the time when the self-intermediate scattering function (Figure 1(b)) decays to e^{-1}. The temperature dependence of the dynamical behavior between self-diffusion coefficient D and the structural relaxation time τ is presented in Figure 1(c). The coupling between D and τ holds well at high temperatures for $T > 1150$ K, but the SE relation breaks down at low temperatures for $T < 1150$ K. With the temperature violation of SE relation being above the glass transition temperature of 860 K (see Figure S1 in the Supplementary Information), the disassociation of the self-diffusion coefficient and the structural relaxation time differs from the pictures of the glass transition.

To understand the mechanism of SE relation breakdown structurally, we studied the structural evolution during the process of quenching a liquid into its glassy state. The atomic configuration data was collected at different temperatures when the system was cooled from 2000 to 300 K at the rate of 10^{12} K/s. The model trained from the SVM enabled us to classify all the atoms into two groups: liquid-like or solid-like. Then, we deduced that two solid-like atoms combines to form a cluster if their distance is less than 3.4 Å this value corresponds to the first minimum in the Cu–Cu pair correlation function at the temperature of 300 K (see Figure S2 in the Supplementary Information). As the temperature decreases from 2000 to 300 K, it is observed that the total number of solid-like clusters increases initially and subsequently reduces (Figure 2(a)). This indicates that small clusters emerge at first and then starts to agglomerate to form bigger clusters when the liquid is cooled below 1330 K. Furthermore, if we take the derivative of the number of clusters with respect to temperature, it can be found that the differential curve shows a peak value of approximately 1140 K (Figure 2(b)). This temperature value is close to 1150 K, which is the temperature below which the SE relation of the system breaks down. The major peak in the change rate means the clusters agglomerated into each other with the fastest merging rate at a temperature of 1140 K. This tremendous aggregation of solid-like clusters may bring significant change to the structural morphology of the system and finally give rise to the breakdown of the SE relation.

We record the size evolution of the largest and the second largest cluster formed by connected solid-like atoms during the cooling process, as well as the total number of solid-like atoms in the system. As shown in Figure 3, the number of solid-like atoms increases from 0 to 10000 (total size of the studied system) as the temperature decreases. The size of the largest cluster almost coincides with the total number of solid-like atoms at low temperatures for $T < 1140$ K; this implies that the largest solid-like cluster will be dominant at temperatures below 1140 K. The size of the second largest cluster (Figure 3, inset) reaches a maximum peak value at a temperature of 1330 K and then shrinks after the peak. These results correspond with the data shown in Figure 2, which shows that at quenching temperature above 1330 K the liquid structure changes due to the number growth of disconnected solid-like clusters but in a low-temperature regime below

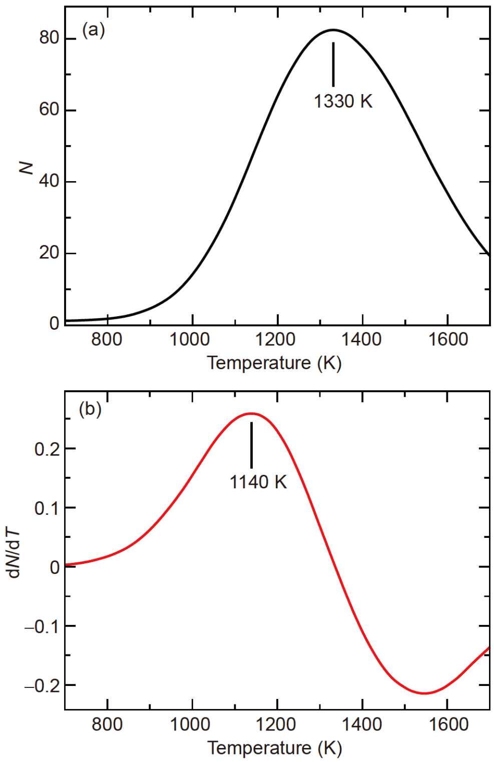

Figure 2 Total number of clusters formed by connected solid-like atoms and its derivative with respect to temperature. (a) The population has a maximum in number occurring at 1330 K; (b) the main peak of the cluster number derivative at 1140 K, which roughly coincides with the temperature where the SE relation breaks down.

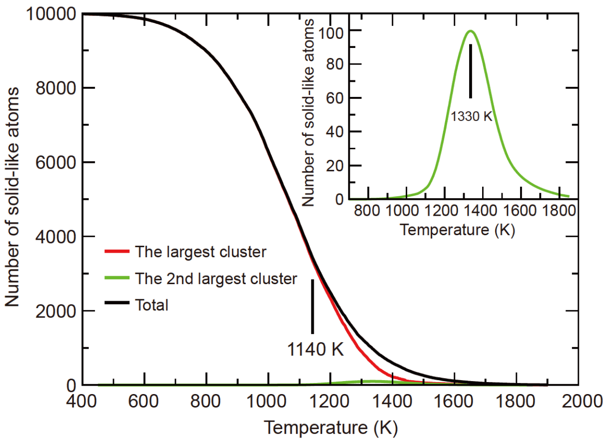

Figure 3 Comparison of the total size of the solid-like atoms in the system with respect to the largest and second largest formed clusters. The size of the largest cluster almost coincides with the total number of solid-like atoms below 1140 K, and the size of the second largest cluster (inset) peaks at 1330 K.

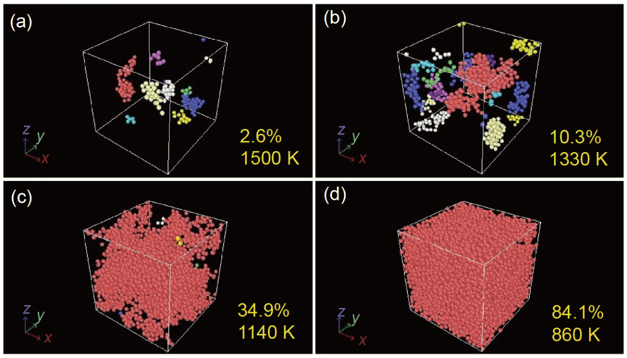

Figure 4 Growth of clusters comprising solid-like atoms in the system. Typical simulation snapshots depicting the growth of clusters at (a) 1500, (b) 1330, (c) 1140, and (d) 860 K (T_g). The percentages show the proportion of solid-like atoms at different temperatures. Different color spheres represent different disconnected clusters.

1140 K, a dominant cluster grows progressively by merging with other small solid-like clusters.

For direct visualization of the solid-like atomic clusters, in Figure 4 we present typical atomic configurations obtained at the temperatures considered during the cooling process. Figure 4(a) shows that at high temperature there are a few uncorrelated small clusters formed by connected solid-like atoms immersed throughout the liquid, and many of them are isolated from each other. Whereas after quenching to T = 1330 K, as illustrated in Figure 4(b), there is a rapid increase in number of solid-like clusters and they consistently grow in size, connect, and merge with each other. The largest cluster spans across the entire system closely at T = 1140 K. The connected solid-like atoms become the dominant population: only a negligible number of solid-like atoms can be found to be separated from the largest connected cluster as in Figure 4(c), and this roughly coincides with the temperature at which the SE relation of the system breaks down. Finally, at the glass transition temperature, the system is fully occupied by the solid-like atoms as shown in Figure 4(d).

4 Conclusion

In conclusion, we investigate the structural evolution and the dynamics of supercooled metallic glass-forming liquids by MD simulation and the machine learning method. The result reveals that the SVM method can be used to classify each atom as liquid-like or solid-like and to investigate the change of the atomic structure. Upon cooling, numbers of isolated small clusters consisting of solid-like atoms emerge out of the liquid in the beginning, and then they grow and join with one another into a single, extensive, connected network of solid-like atoms. We find that the SE relation breaks down when the size of the largest solid-like cluster enlarges rapidly by consuming other small clusters at the fastest rate, as expected there is a connection between the atomic structure of glass-forming liquid and its dynamics. Our results show that the decoupling between the transport coefficients D and the structural relaxation time τ can be interpreted in terms of rapid changes in the atomic structure, which provides new insight into the study for characterizing anomalous dynamics of glass-forming liquids.

We thank all members of the Beijing Metallic Glass Club for the long-term useful discussions. This work was supported by the National Natural Science Foundation of China (Grant Nos. 11804027, and 11525520), the National Basic Research Program of China (Grant No. 2015CB856801), and the Fundamental Research Funds for the Central Universities (Grant No. 2018NTST24).

Supporting Information

The supporting information is available online at phys.scichina.com and link.springer.com. The supporting materials are published as submitted, without typesetting or editing. The responsibility for scientific accuracy and content remains entirely with the authors.

1 P. G. Debenedetti, and F. H. Stillinger, Nature **410**, 259 (2001).

2 W. H. Wang, Prog. Mater. Sci. **106**, 100561 (2019).

3 J. C. Qiao, Q. Wang, J. M. Pelletier, H. Kato, R. Casalini, D. Crespo, E. Pineda, Y. Yao, and Y. Yang, Prog. Mater. Sci. **104**, 250 (2019).

4 Z. W. Wu, W. Kob, W. H. Wang, and L. Xu, Nat. Commun. **9**, 5334 (2018), arXiv: 1808.04084.

5 P. Luo, Y. Z. Li, H. Y. Bai, P. Wen, and W. H. Wang, Phys. Rev. Lett. **116**, 175901 (2016).

6 T. Scopigno, G. Ruocco, F. Sette, and G. Monaco, Science **302**, 849 (2003), arXiv: cond-mat/0311305.

7 L. Wang, A. Ninarello, P. Guan, L. Berthier, G. Szamel, and E. Flenner, Nat. Commun. **10**, 26 (2019), arXiv: 1804.08765.

8 T. Kawasaki, and K. Kim, Sci. Adv. **3**, e1700399 (2017), arXiv: 1701.06028.

9 Y. C. Hu, F. X. Li, M. Z. Li, H. Y. Bai, and W. H. Wang, J. Appl. Phys. **119**, 205108 (2016).

10 R. Soklaski, V. Tran, Z. Nussinov, K. F. Kelton, and L. Yang, Philos. Mag. **96**, 1212 (2016), arXiv: 1502.01739.

11 L. Xu, F. Mallamace, Z. Yan, F. W. Starr, S. V. Buldyrev, and H. Eugene Stanley, Nat. Phys. **5**, 565 (2009).

12 S. Sastry, and C. Austen Angell, Nat. Mater. **2**, 739 (2003).

13 F. H. Stillinger, and J. A. Hodgdon, Phys. Rev. E **50**, 2064 (1994).

14 G. Tarjus, and D. Kivelson, J. Chem. Phys. **103**, 3071 (1995).

15 S. R. Becker, P. H. Poole, and F. W. Starr, Phys. Rev. Lett. **97**, 055901 (2006), arXiv: cond-mat/0605170.

16 S. Pan, Z. W. Wu, W. H. Wang, M. Z. Li, and L. Xu, Sci. Rep. **7**, 39938 (2017).

17 S. S. Schoenholz, E. D. Cubuk, D. M. Sussman, E. Kaxiras, and A. J. Liu, Nat. Phys. **12**, 469 (2016).

18 Y. T. Sun, H. Y. Bai, M. Z. Li, and W. H. Wang, J. Phys. Chem. Lett. **8**, 3434 (2017).

19 S. Plimpton, J. Comput. Phys. **117**, 1 (1995).

20 M. I. Mendelev, D. J. Sordelet, and M. J. Kramer, J. Appl. Phys. **102**, 043501 (2007).

21 W. Kob, and H. C. Andersen, Phys. Rev. E **52**, 4134 (1995), arXiv: cond-mat/9505118.